Received: 16 July 2021 | Revised: 20 May 2022 | Accepted: 21 May 2022

DOI: 10.1111/jace.18638

Journal of the American Ceramic Society

RESEARCH ARTICLE

Powder-fed directed energy deposition of soda lime silica glass on glass substrates

Fiona Spirrett[1] | **Kyriaki Corinna Datsiou**[1] | **Marlin Magallanes**[2] | **Ian Ashcroft**[1] | **Ruth Goodridge**[1]

[1]Centre for Additive Manufacturing, Faculty of Engineering, University of Nottingham, Nottingham, UK

[2]Glass Technology Services Ltd, Chapeltown, Sheffield, UK

Correspondence
Ruth Goodridge, Centre for Additive Manufacturing, Faculty of Engineering, University of Nottingham, Nottingham NG8 1BB, UK.
Email: ruth.goodridge@nottingham.ac.uk

Present address
Fiona Spirrett, Joining and Welding Research Institute, Osaka University, Suita, Japan.
Kyriaki Corinna Datsiou, Department of Engineering and Technology, University of Hertfordshire, Hatfield, Hertfordshire, UK.

Funding information
EPSRC (Engineering and Physical Sciences Research Council, UK) Centre for Doctoral Training in Additive Manufacturing and 3D Printing, Grant/Award Number: EP/L01534X/1; Glass Technology Services

Abstract

Novel glass processing by powder-fed directed energy deposition was explored as a method of adding glass décor to glass surfaces and bottles. Consistent, semi-transparent, single-line tracks of soda lime silica glass could be processed onto glass substrates of the same composition, without significant cracks forming in the substrate. A suitable processing window was found with laser power and scan speed showing independent effects on processing. Consideration of processing surface conditions and reduction of laser transmission through transparent substrates was necessary, and the use of an adhesive tape layer aided adhesion of glass feedstock to substrate surfaces. The work demonstrates the potential for a one-step method of glass bottle decoration for the packaging industry, with scope to create 3D designs of high geometric complexity and customizability on glass substrates, thereby adding value to glass packaging by brand differentiation without the high costs associated with molds and tooling.

KEYWORDS
additive manufacturing, directed energy deposition, glass, laser, powder, soda lime silica

1 | INTRODUCTION

Glass is extensively used in a wide range of industries due to its high chemical resistance, durability, and esthetic appeal. Traditional glass decoration methods include techniques such as embossing, engraving, and etching. Laser engraving applies decorative features onto the surfaces of glass objects with a laser (typically Nd:YAG pulsed),[1] whereas conventional engraving works by abrading glass surfaces using small abrasive wheels and drills, or diamond-tipped burrs. However, these decorations are often opaque in nature, and the processes impart stresses, creating or exaggerating defects that can cause cracking or fracturing. Embossing glass objects to impart decoration involves the use of molds. For this, the customization of design is limited, as each new design requires a new mold, increasing associated costs. Fabrication of customized glass packaging by glass molding in small production volumes may, therefore, incur greater costs than other methods. Chemical wet etching, while low cost, shows poor repeatability and has risks associated with chemical contamination.[2] Many of these techniques

require multiple production steps to fabricate a customized end-product, whereas additive manufacturing (AM) could be used to fabricate bespoke glass products in a single step with no added cost for customization.

Glass-AM offers an alternative method for glass decoration, with the benefit of high geometric freedom, making the fabrication of bespoke glass items possible at efficient cost.[3] A number of AM techniques have been investigated for glass processing; however, little progress has so far been made in glass-on-glass AM, with much of the literature reporting processing of glass onto ceramic substrates, or methods requiring multiple processing and post-processing steps. For example, Nguyen et al. demonstrated AM of silica inks by direct ink writing to produce transparent glass objects; however, the shrinkage of parts during post-process densification was reported.[4] Although shrinkage is expected during sintering, this needs to be accounted for in the model design to achieve accurate part dimensions. Further, Dylla-Spears et al. described the challenges faced during the fabrication of transparent silica parts with gradient refractive index by direct ink writing and demonstrated the fabrication of simple geometries that required polishing for optical applications.[5] Multistep AM processing of glass has also been reported by Kotz et al., fabricating complex, transparent parts from silica inks by stereolithography (SLA) and two-photon polymerization.[6,7] Some of the challenges reported included the shrinkage of parts during post-process heat treatments and difficulties removing uncured material from hollow structures for SLA. These AM techniques require thermal post-processing steps in order to achieve densification and remove non-glass substituents, often resulting in volumetric shrinking, reducing the geometrical accuracy of parts, and increasing manufacturing time and cost.

Single-step AM methods have been used to process glass-on-ceramic substrates. Klein demonstrated material extrusion of molten glass through a ceramic nozzle in a layer-by-layer manner to fabricate optically transparent, decorative glass parts.[8] However, the achievable resolution of parts was limited by layer thickness and nozzle diameter. Glass-on-glass processing was not demonstrated using this method, as parts were built on a ceramic substrate to deliberately reduce adhesion at annealing temperatures to allow removal of parts.[9]

The potential benefits of powder bed fusion methods of AM have been demonstrated for glass processing in a small number of publications. Datsiou et al. demonstrated the processing of soda lime silica glass powder by selective laser melting (SLM) onto a ceramic substrate and optimized parameters for fabrication of parts with high geometrical complexity, such as lattices.[10] However, the parts produced were opaque due to the presence of unfused powder on the surface of the structures and high internal porosity. The process involved removing the glass structures from the ceramic substrate. Datsiou et al. further evaluated SLM-processed glass parts, revealing a flexural strength of between 6 and 7 MPa for $1 \times 2 \times 8\text{-mm}^3$ structures.[11] The feasibility of processing quartz glass by SLM was investigated by Khmyrov et al., reporting limited success in processing glass on substrates of the same composition.[12] Further work achieved crack-free processing of quartz glass on glass substrates, likely thanks to the extremely low coefficient of thermal expansion (CTE) of quartz glass composition ($0.5 \times 10^{-6}\,°C^{-1}$)[13] avoiding cracking caused by thermal stress.[14] Comparatively, soda lime silica glass, with a much higher CTE of $9 \times 10^{-6}\,°C^{-1}$,[15] has been reported to be much more susceptible to thermal shock during laser treatment.[16] Fateri and Gebhardt reported the challenges of processing soda lime silica, the common composition for drinkware and bottles, by SLM, but did not investigate the processing of glass onto a glass substrate.[17] Opaque, decorative pieces were fabricated for jewelry applications.[18] The feasibility of processing borosilicate glass by SLM was demonstrated by Eichler et al., again experiencing adhesion of loose powder to part surfaces due to the dissipation of heat energy within the powder bed and requiring a post–heat treatment to improve the surface finish.[19] The reduction in geometrical accuracy caused by the dissipation of energy through a melt pool in powder bed fusion of glass was also noted by Luo et al., who also observed a reduction in transparency caused by bubble formation.[20]

Directed energy deposition (DED) is a single-step process using a high-powered laser to melt wire or powder feedstock as they are deposited on to a suitable substrate. The wire-fed approach to DED processing of glass filaments has so far demonstrated simple geometries of soda lime silica, borosilicate, and quartz onto a glass substrate. Thermal stress and cracking were avoided by employing a heated stage; however, the resolution of parts was limited by filament size, and the demonstrated geometries were limited to walls and simple deposits.[21] von Witzendorff et al. presented continuous and discontinuous processing of quartz glass filaments by DED, and similarly simple geometries were demonstrated.[22] Melting of 2-mm borosilicate glass filaments has also been described by Capps et al., by a digital glass forming method.[23] CO_2 laser irradiation was used to melt the glass filament onto a borosilicate substrate heated to 450°C. Transparent structures were fabricated; however, resolution and geometric complexity appeared to be limited by the large filament size. Powder feedstock can be used instead of filaments in DED to improve resolution; however, to the authors' knowledge, DED of glass powders has not been explored in the available literature.

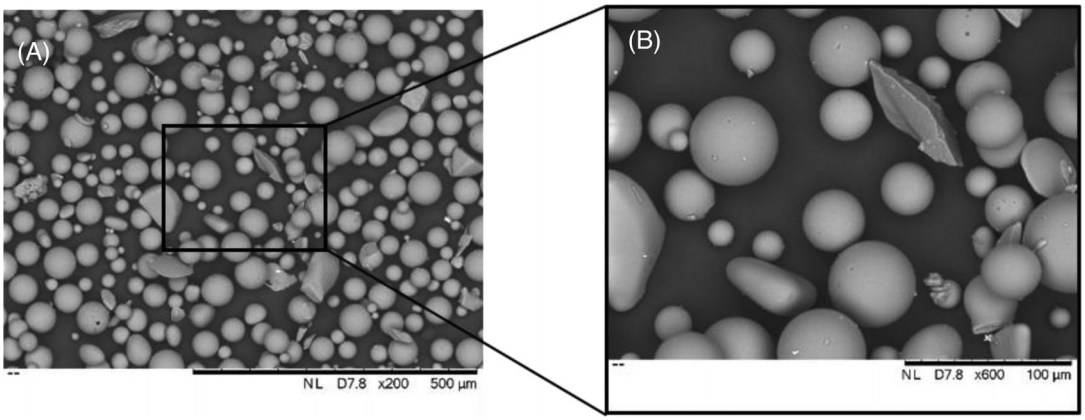

FIGURE 1 Scanning electron microscopy (SEM) micrographs of SLSG-C glass feedstock at (A): 200× magnification and (B): 600× magnification

This study has therefore investigated novel glass processing by powder-fed DED, processing soda lime silica glass powder onto a substrate of the same composition. Soda lime silica is a common glass composition used in applications requiring transparency, and durability, but not requiring as much resistance to thermal shock as other compositions such as borosilicate. For this reason, it is a popular composition for glass bottles and drinkware as it is cost-effective and meets all physical requirements. Developing AM processing for soda lime silica glass would allow it to be used for the decoration of glass items. This composition also has a low melting point and glass transition temperature with a wide working range relative to other glass compositions, allowing processing at lower energy densities. The initial focus of this study was on producing single-layered glass tracks on 1-mm substrates, before progressing to more complex structures and processing onto substrates of 4-mm thickness, and then curved bottle surfaces with varying wall thickness. Ultimately, this study explores the possibility of utilizing powder-fed DED to add value in the glass packaging industry, with potential exploitation for other applications or fabrication of complex, 3D glass parts.

2 | EXPERIMENTAL DESCRIPTION

2.1 | Material characterization

Soda lime silica beads ($73SiO_2$, $13Na_2O$, 9CaO, 4MgO, and $1Al_2O_3$), "SLSG-C" were characterized for DED investigations (supplied by Glass Technology Services Ltd, UK). The feedstock was imaged by scanning electron microscopy (SEM) (TM3030, Hitachi, Japan) and measured by laser diffraction (Mastersizer 3000, Malvern, UK) to determine an average particle size (Dv50) and particle size distribution (PSD). SLSG-C presented as a fine, spherical powder with some irregular particles within the sample (Figure 1). Average particle size was measured as Dv50 = 45 μm and PSD as 23–63 μm. The sample demonstrated a Gaussian PSD, with a relatively wide distribution, which is potentially problematic as a large quantity of fine particles can reduce the flowability of a powder due to high interparticulate forces between smaller particles.[24]

Basic flowability energy (BFE), specific energy (SE), and flow rate index (FRI) were measured by powder rheometry (FT4 Powder Rheometer, Freeman Technology, UK) to determine flow characteristics. BFE is a measure of total energy (mJ) and relates to the energy required for the material to flow under confined conditions, akin to those in a powder bed. SE is a measure of the energy required for material to flow under non-confined flow (mJ/g), which is applicable to material being delivered through a nozzle. FRI is a measure of sensitivity to flow rate and represents the cohesiveness of a powder (i.e., the attractive interactions among particles due to surface energies and Van der Waals forces). SLSG-C showed a high FRI value (1.16), suggesting significant cohesion due to high inter-particulate forces among fine particles. This material also had a BFE of 172 mJ, and an SE of 2.22 mJ/g, higher values than those measured for larger PSDs with better flow characteristics, suggesting a reduced flowability in confined and non-confined environments. Further material data is available in the Supporting Information section. Laser absorbance at the wavelength of interest, 1070 nm, was measured by UV–Vis and Fourier transform infrared (FTIR) spectroscopy with an absorbance of $A = 0.39\ cm^{-1}$.

2.2 | DED system

A custom-made, modular DED system at the University of Nottingham was used for this work (Figure 2). This setup incorporated a laser, a material feeder, multiple material

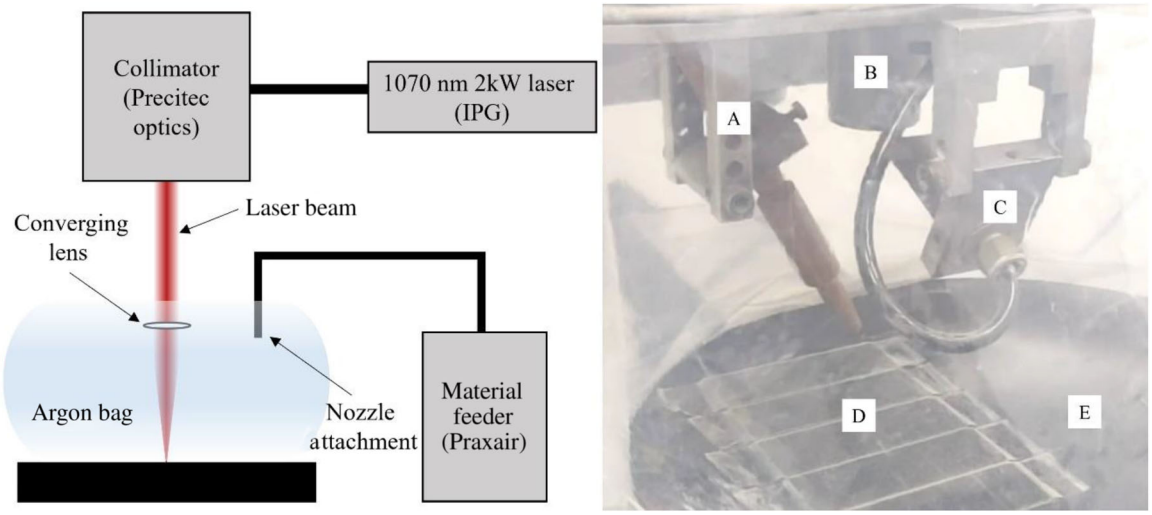

FIGURE 2 Schematic diagram of the directed energy deposition (DED) processing setup and photograph of the side-nozzle delivery setup: (A) lateral powder nozzle, (B) laser, (C) argon nozzle, (D) glass substrates affixed to base plate, and (E) darkened base plate

feedstock nozzles, and a translational stage. A CW Yb fiber laser (IPG Photonics, USA) that operates at a wavelength of 1070 nm and has a spot size of 1 mm at focus was used to process the soda lime silica material described in Section 2.1. The laser operates up to 2-kW power and was used in conjunction with a multi-axis stage (Zaber, USA), capable of translation in the *x*- and *y*-directions with speeds of up to 100 mm/s. The multi-axis stage was controlled via a computer program, through which G-code files could be translated. The process of file preparation involved the creation of specific features, such as straight lines, curves, and a combination of both, using a 3D CAD package, SOLIDWORKS (Dassault Systèmes, FR), and editing of the STL file to give single layers written in G-code. The laser was mounted on a *z* axis for multilayer processing. Different feedstock delivery attachments were available, a 1-mm coaxial nozzle, and a 2-mm side nozzle, for powder feed. An automatic powder feeder (Model 1264, Miller Thermal Inc, USA) was used in conjunction with the powder nozzles, able to vary carrier gas pressure (L/min) and powder flow rate (powder wheel speed—rpm). An argon bag was used for shielding and containment of powder. Soda lime silica glass substrates of varying thickness (1, 4, and 5–7 mm) were mounted to the stage for processing.

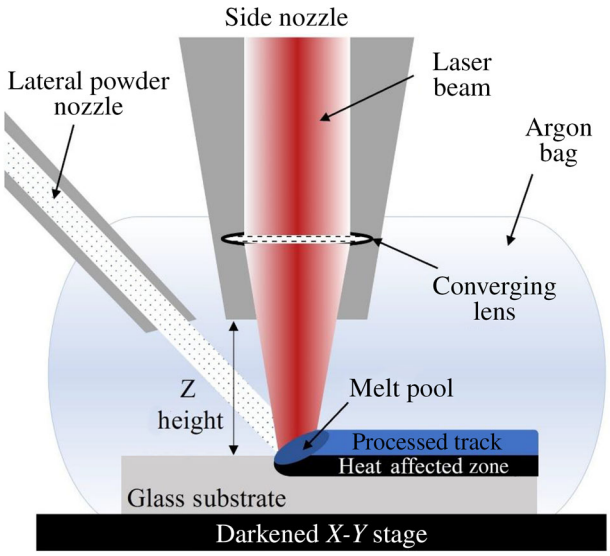

FIGURE 3 Schematic representations of side-nozzle configurations for directed energy deposition (DED) processing

2.3 | Experimental setup

2.3.1 | Feedstock delivery system

An automatic powder feeder was used with two separate nozzle attachments (Figure 4). Powder was delivered by a volumetric feed principle, whereby powder was rotated and collected in small slots and then metered into a powder hose and delivered to the nozzle. Control of rpm determined the rate at which powder flowed to the nozzle. Off-axis nozzles are easy to use but have been reported to result in varying deposit height dependent on scan direction with relation to the direction of powder delivery. Alternatively, coaxial nozzles can provide better powder capture rates and are not affected by scan direction, making them more suited for multilayer processing.[25] For side powder delivery, a custom-made copper nozzle with a 3-mm orifice was lined with a 2-mm Teflon tube and positioned at 27.5° relative to the laser beam (Figure 3). A coaxial nozzle mounted on the *z* axis was also tested, whereby powder was delivered to a copper nozzle with an

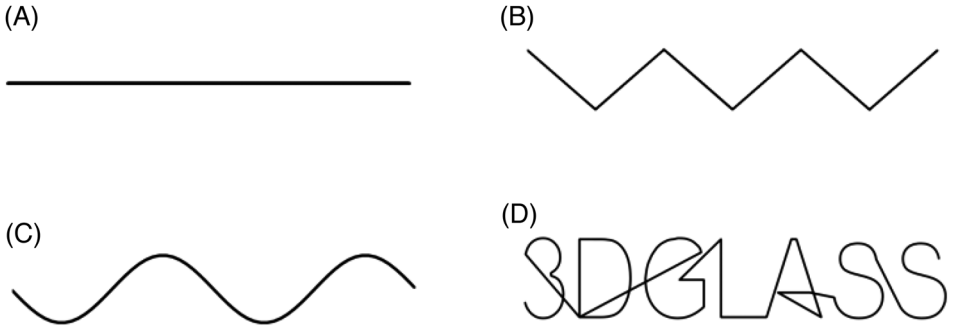

FIGURE 4 Design geometries: (A) single tracks, (B) straight features, (C) curved features, and (D) text design

annular orifice, converging streams of powder at the laser focal point. Despite the nozzle diameter being 1 mm, the coaxial design restricted powder flow. Glass powder feedstock was dried in a furnace at 100°C before investigations to remove moisture and aid flow of powder through the delivery system. The powder was delivered to the substrate through one of the nozzles at varying carrier gas (Ar) flow rates (5–10 L/min) and speeds (1–12 rpm), determining the powder flow rate. Powder flow rate (g/s) was measured for delivery of SLSG-C via the two nozzle attachments, in order to determine suitable feed parameters for glass powder processing by DED.

2.3.2 | Glass substrate considerations

Soda lime silica glass plates of varying thicknesses (1-mm microscope slides, 4-mm glass plates, and 5–7-mm bottle surface) were used as substrates in order to match the CTE of the feedstock, to aid adhesion, and reduce the risk of thermal shock. The influence of mild heating (~100°C) of 1-mm glass substrate to reduce thermal shock was also of interest, and a substrate heater was employed for one of the processing trials. The transparent glass substrates were highly transmissive to the near IR laser wavelength (1070 nm) in use. To address this, modification of the base plate underneath the glass substrates and the glass substrates themselves was undertaken. Three base plates were considered upon which the glass substrates were fixed. These were an aluminum plate, a grit-blasted aluminum plate darkened by graphite, and a black anodized plate. Darkened base plates were selected as they were expected to reduce reflectance and act as a heat source (as transmitted energy is absorbed), improving glass processing by reducing temperature gradients. Additionally, modification of the glass substrates involved the application of a layer of adhesive cellophane tape on their surfaces to improve the laser absorption of glass feedstock on to the glass substrate. For glass bottle substrates, removable matt-black paint was applied to the inside surface of the bottle. 1-mm glass substrates were used for process parameter investigations for process mapping and initial testing of different geometries. Glass substrates measuring 4 mm were expected to have higher resistance to thermal shock compared to 1-mm substrates and were used to demonstrate the processing of complex geometries. Glass bottle substrates were used to demonstrate the application of DED processing for glass packaging décor.

2.4 | Process parameters

The main parameters investigated for their effect on glass processing were feedstock delivery, energy density (ED), and design geometry. Investigations were carried out to test different combinations of parameters for processing different geometries on glass substrates of varying thicknesses. Resulting structures were assessed based on glass consolidation and substrate cracking. Process mapping was used to inform process parameters for testing various geometries and substrate thickness going forward.

2.4.1 | Feedstock delivery parameters

Glass powder material was delivered through a 2-mm side nozzle and a 1-mm coaxial nozzle. Glass feedstock was delivered to a confined pot and measured at 10-s intervals. The average mass delivered per second was recorded for each nozzle at various carrier gas flow rates (L/min) and powder wheel speeds (rpm). This helped to define an optimal mass deposition rate for consistent delivery of glass powder feedstock.

Powder wheel speed was varied between 1 and 12 rpm, and the resulting structures were observed by SEM. Average deposit height was measured by digital calipers. Results were used to define suitable parameters for supplying a consistent quantity of glass material to produce parts of consistent deposit height by DED processing.

2.4.2 | Energy density

Laser power and scan speed are important process parameters as they control the energy delivered to the feedstock powder. The following equation shows the relationship between ED (J/mm^2), laser power (P, W), and scan speed (v, mm/s) (layer thickness [t] assumed to be 1 mm):

$$ED = \frac{P}{v \times t} \quad (1)$$

where ideal parameters for processing require a high enough ED to result in consolidation and adhesion of melted glass feedstock onto the glass substrate, but not so high to cause cracking and fracturing of parts or substrates from thermal shock. Efforts to define a suitable processing window that fulfills these requirements were made by testing a range of combinations of these parameters, with scan speed between 500 and 700 mm/min, and laser power between 95 and 130 W. Single tracks of soda lime silica were processed and used to populate a process map. Processed structures and substrates were assessed through SEM and X-ray computed tomography (XCT) (MCT225, Nikon Metrology NV, JP).

2.4.3 | Laser focal position

The effect of laser focal position on glass powder processing was investigated. The laser used during this study was affixed to a mount able to move translationally in the z axis (vertically). The z height was adjusted to change the focal point of the laser in relation to the substrate. This directly impacts the laser spot size and, therefore, the energy input during processing. Focal position was investigated at focus ($F = 0$) and up to 3-mm out of focus ($F = -3$ to $F = +3$). Corresponding spot sizes can be estimated from previous beam profiling of the laser system. D86 values, the diameter of the circle at the centroid of the laser beam profile containing 86% of the power, were estimated as 0.9 mm at $F = 0$, increasing to 0.956 mm at $F = 2$ and 1.068 mm at $F = 4$. Tracks of soda lime silica feedstock were processed at 10 and 11 J/mm^2 on a 1-mm glass substrate, and average deposit height was measured by digital calipers. Results were used to determine a suitable laser focal position for glass processing by DED.

2.4.4 | Design geometry

Simple geometries (single tracks, straight features) were written directly in G-code (incremental). More complex geometries (text designs) were created using a CAD package (SOLIDWORKS, Dassault Systèmes, FR), converted to G-code (absolute coordinate), and edited for single-layer processing. The selected geometries reflected features of interest for glass decoration, including straight features, curved features, and text using a combination of curves and straights. The four designs used are visualized in Figure 4. The designs were confined to 60 × 20 mm to accommodate processing onto a glass substrate of 70 × 25 × 1 mm. These designs were processed onto glass substrates of different thicknesses, and the effect of design feature on DED of glass powder was investigated.

3 | RESULTS

3.1 | Experimental setup

3.1.1 | Feedstock delivery system

Average masses of powder delivered via a coaxial nozzle and a lateral nozzle were measured for soda lime silica glass feedstock. Delivery of fine soda lime silica powder (SLSG-C, PSD = 23–63 μm) through the coaxial nozzle was inconsistent. This was due to the sensitivity of the coaxial nozzle to powder flowability and cohesion. Fine particles gathered in the powder chamber, preventing a consistent flow of glass powder through the nozzle. Using powder feed parameters of 5 L/min carrier gas flow, and 2-rpm wheel speed, the coaxial nozzle delivered 3.3 mg/s of SLSG-C, an insufficient quantity for DED processing.

Using the same powder feed parameters, the 2-mm copper side nozzle delivered SLSG-C feedstock at a feed rate of 23 mg/s. This nozzle was less sensitive to material flowability than the coaxial nozzle; however, electrostatic interaction between the copper nozzle and the glass feedstock reduced the consistency of powder delivery. A copper nozzle with a Teflon lining (2-mm diameter) was utilized to reduce this effect. Powder delivery became more consistent and the average mass delivered increased to 39 mg/s. This was the preferred powder feed setup for the investigations previously outlined.

3.1.2 | Substrates

Little to no deposition and adhesion of the glass was observed on uncoated soda lime silica glass substrates during processing. However, the application of a single layer of cellophane tape on the glass substrate was found to considerably improve the deposition and adhesion of glass powder feedstock to the substrate. This was attributed to localized heating when the cellophane tape layer was irradiated and vaporized by the laser, allowing glass powder to

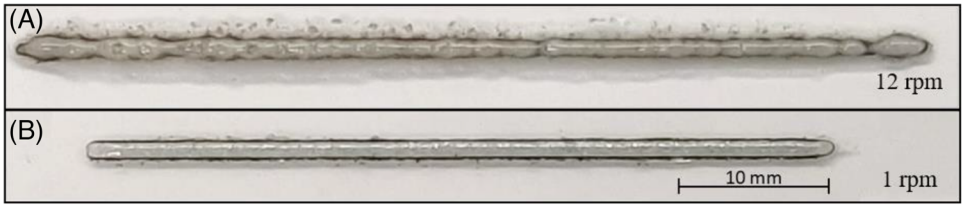

FIGURE 5 Glass deposits on glass substrate at varying feed rates (energy density [ED] = 11 J/mm^2): (A): 12 rpm, (B) 1 rpm

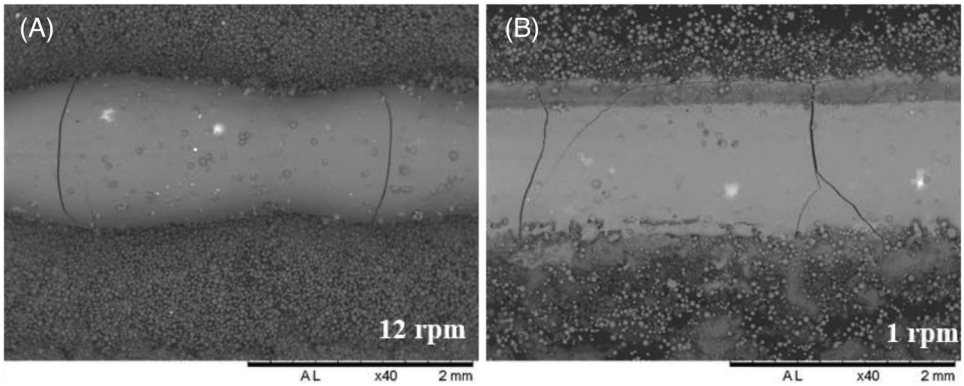

FIGURE 6 Scanning electron microscopy (SEM) micrographs of glass deposits at (A) 12 rpm and (B) 1 rpm, showing variation in deposit width

absorb energy from the heat-affected zone and eventually melt on to the substrate during processing.

The thickness of the glass substrates was also found to affect DED of glass. Substrates of 1-mm thickness suffered from thermal shock when processed at certain energy densities, causing microcracks to propagate laterally on the top surface of the substrate, along the deposited glass tracks. Thicker glass substrates (100 × 100 × 4 mm) and bottles with a varying wall thickness of 5–7-mm thickness showed a higher thermal shock resistance under the same conditions, minimizing crack formation and propagation.

Glass deposition during DED was also found to depend on the base plate beneath the substrates. Laser absorption of glass powder was low when the glass substrate was fixed to an aluminum base. Laser radiation was transmitted through the transparent glass feedstock and substrate and was reflected by the aluminum surface. No deposition of glass was therefore observed. Using a black anodized base plate or a graphite-darkened surface (and matt black paint coating for the inside of bottle substrates) was observed to improve processing. This is thought to be explained by the absorption of laser energy at the base plate, increasing the temperature of the substrate and conducting heat to the glass feedstock. As the energy absorptivity of the glass powder increases with temperature, this heat conduction could lead to glass feedstocks self-heating, further increasing absorptivity. These darkened base plates also acted as a heat sink to prevent thermal runaway during processing. Glass feedstocks were melted consistently onto glass substrates above these darkened base plates. As absorption by glass powder is usually greater than that of solid materials, glass substrates did not melt from laser processing.

3.2 | Process parameters

3.2.1 | Feedstock delivery parameters

Powder wheel speed was varied to investigate the effect of glass powder processing by DED. Single tracks were processed at varying speeds. At high rpm, a larger quantity of glass feedstock was delivered to the substrate compared to low rpm. The resulting glass deposits during processing at a high speed (12 rpm) showed an average deposit height of 0.9 mm with significant variation in deposit height (to one standard deviation), compared to low speed (1 rpm) processing, which resulted in an average deposit height of 0.2 mm and consistent height (to one standard deviation). Deposit height was measured with digital calipers across multiple samples. Figure 5 shows the resulting glass deposits under conditions of A: 12 rpm and B: 1 rpm, and SEM micrographs of these samples are shown in Figure 6. The inconsistent width of the deposited glass tracks at 12 rpm compared to 1 rpm can be seen.

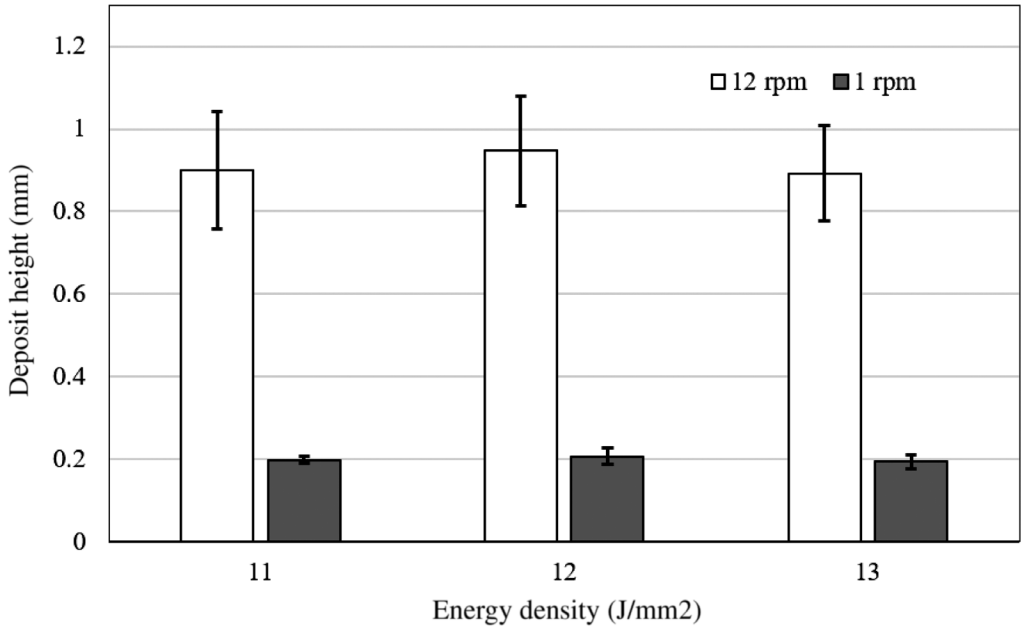

FIGURE 7 Average deposit height of glass tracks at varying process parameters (one standard deviation)

Deposit height was compared at 12 and 1 rpm across three different energy densities. No significant difference was found in deposit height between 11 and 13 J/mm^2. Figure 7 displays these results to one standard deviation. Based on the lower variation in deposit boundaries at lower feed rates, and for delivery of sufficient powder, feed parameters of 1 and 2 rpm (powder wheel speed) and 5 L/min (carrier gas flow) are recommended.

3.2.2 | Energy density

The investigation of ED, described in Section 2.4.2, was unsurprisingly found to be one of the key factors for feedstock consolidation in DED of glass powder. Laser power and scan speed were varied to define a suitable processing window. ED was varied between 8 and 15 J/mm^2, and effects were assessed based on certain observations: (a) if the glass substrate fractured or remained intact, (b) if the glass powder feedstock melted and deposited onto the substrate, and (c) the consistency of the deposited glass. A process map was populated relating ED and success or failure of processing (Figure 8).

The process map shows the effect of laser power and scan speed combinations on the processing of SLSG-C by this method. An effective "processing window" was found between energy densities of 10–13 J/mm^2. In general, these combinations of scan speed and laser power largely resulted in consistent, well-consolidated single tracks of glass deposits, and under these conditions, 1-mm glass substrates did not suffer significant cracking from thermal stress. Occasions where processing among these energy densities did not result in consistently deposited glass tracks or suffered thermal shock are evident.

Cracking of substrates occurred only at or above 115 W, whereas inconsistent consolidation of glass was seen most commonly below 11 J/mm^2, where we can assume the absorption of laser energy by the glass powder was insufficient for glass melting due to low ED. ED was used to relate laser power and scan speed into one numerical value; however, these results suggest that laser power and scan speed had independent effects on glass processing.

Processing of single tracks of SLSG-C on 1-mm substrates was most successful at around 11.5–12.5 J/mm^2, at laser powers below 115 W. However, this process map is only relevant for this combination of variables. For different compositions of glass, different substrate thicknesses, and different scan designs, process maps would differ. The required energy for full consolidation of glass on glass substrates changed depending on these factors. For example, thicker substrates required an increase in ED, through the increase of laser power or decrease in scan speed, in order to achieve consolidation of glass powder on the substrate surface, and more complex scan designs required a decrease in ED to protect the substrate from thermal shock due to a buildup of energy in areas of high stress concentration (Section 3.2.3).

Microcracks were visualized by micro-XCT. Cracks appeared to initiate from the top surface of the glass, adjacent to processed glass tracks, penetrating ~0.5 mm into

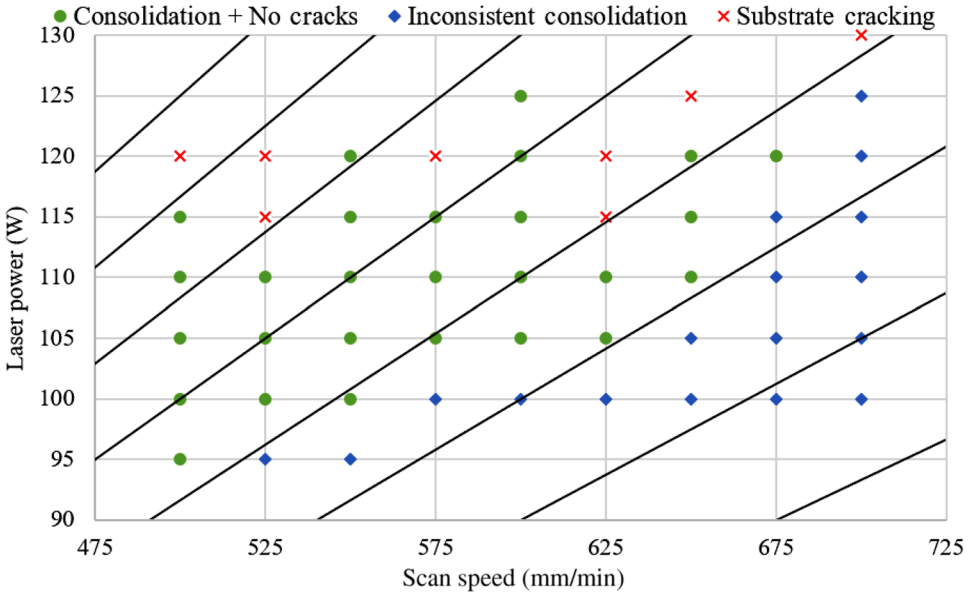

FIGURE 8 Process map for single tracks of SLSG-C (23–63 μm) on a 1-mm substrate of the same composition. Trend lines depict the energy density at different combinations of laser power and scan speed. Crosses represent substrate cracking, diamonds represent inconsistent consolidation, and circles represent consistent deposition of glass and the absence of substrate cracking.

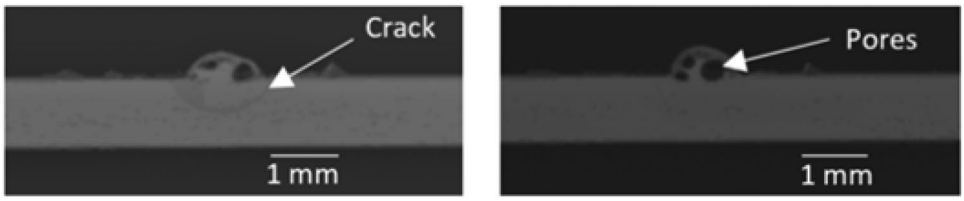

FIGURE 9 A cross section of a directed energy deposition (DED)-processed glass sample (12 J/mm^2) showing crack formation and internal porosity

the glass substrate. These were visible by eye through the bottom surface of samples. Evidence of porosity within the processed glass tracks was also seen through micro-XCT (Figure 9).

3.2.3 | Laser focal position

Processing of single tracks was carried out at 10 and 11 J/mm^2, at varying focal positions ($F < 0$, $F = 0$, and $F > 0$). Processing at $F < 0$ was unsuccessful, with melting and consolidation of glass feedstock not observed. At focal positions of $F = 0$ and $F > 0$ (1–3 mm), glass feedstocks melted consistently. A difference was observed in the deposit height of processed glass based on the laser focal position (Figure 10). The more out of focus, the smaller the average deposit height. This is explained by the decrease in ED relating to a larger spot size area when processing out of focus. Similarly, the effect of ED was observed once again, showing a general increase in deposit height with increased ED.

3.2.4 | Design geometry

Design geometry had a large impact on the success of glass powder processing by DED. Using an ED of 11.5 J/mm^2, processing of a single track resulted in the successful consolidation and deposition of glass feedstock, without substrate fracture. Single-track processing was deliberately carried out in the center of the glass substrates, avoiding the edges where stress concentrations are higher.

For the more complex designs of straight features and curved features, in order to achieve consistent glass feedstock consolidation in these geometries, ED had to be altered. Straight features required a higher ED (12.0 J/mm^2) and curved features required a lower ED (9.24 J/mm^2) for consistent glass powder consolidation. Due to these geometries utilizing movement in multiple axes, two explanations are considered for the altered ED requirements. First, the angle of powder delivery in relation to processing direction, and second, the acceleration and deceleration of stage motors during directional changes affecting the scan speed.

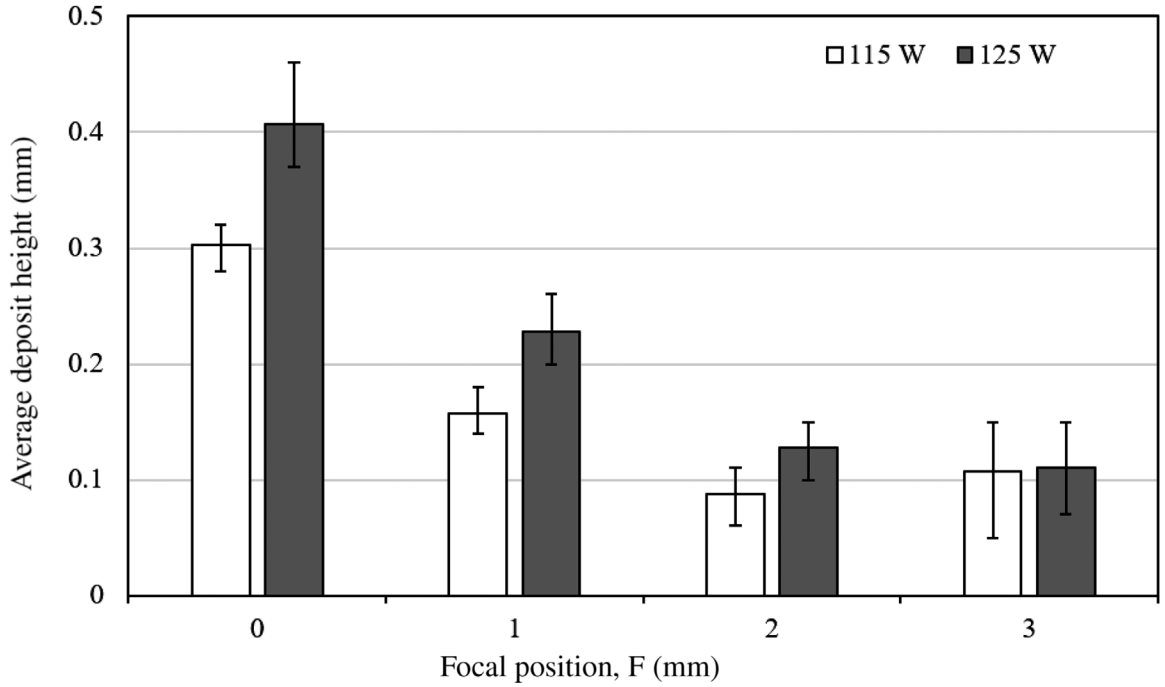

FIGURE 10 Average deposit height by laser focal position at 10- and 11-J/mm^2. Error bars display one standard deviation.

Unlike in straight track processing, cracking of 1-mm substrates was unavoidable for these geometries. Cracking initiated at the apex of curves and the points of directional change, where stress concentrations were higher. As these geometries covered a larger area of the 1-mm substrates, cracking was expected when processing occurred closer to the weaker substrate edges.

For text designs, incorporating both straight and curved features, scan speed was altered accordingly to account for these changes during processing. For curved features, scan speed was increased to consequently decrease ED. For straight features, and particularly those that traveled perpendicularly to the incident of powder delivery, scan speed was decreased in order to increase the ED. Additionally, scan speed was increased to 100 mm/s between features to inhibit glass melting, and pauses were incorporated into the G-code to allow for laser dwell time before initiating glass melting. Processed structures and their corresponding process parameters are shown in Figure 11.

For the text design, energy densities between 9.2 and 13.3 J/mm^2 were used to successfully process the design with consistent glass deposition observed for each feature. Pauses of 0.5–0.7 s were used after instances of max travel speed (in between features). Cracking was unavoidable for processing on 1-mm glass substrates due to the increased stress concentrations associated with the more complex design, as expected. The design was successfully processed onto a 4-mm glass substrate without fracture, due to its higher resistance to thermal shock.

3.2.5 | Demonstration of glass bottle décor application by glass powder DED

For curved bottle surfaces (5–7-mm thickness), an increase in the ED (relative to substrates of 4 and 1 mm) was well tolerated and allowed consistent consolidation of glass powder on the substrate surface. Thermal shock was avoided, and substrates did not fracture. Curved features design was processed at 9.68 J/mm^2 and straight features at 13.25 J/mm^2 (Figure 12).

Variation in deposit height across processed structures was observed, caused by inconsistencies in powder feed. When insufficient powder was delivered to the substrate/laser beam, the inside surface of the bottle substrate showed microcracking, due to excess laser energy being absorbed by the black paint coating.

3.3 | Inspection of deposited glass

To further assess the nature of the deposited glass, X-ray diffraction (XRD) and FTIR were carried out. To assess the crystallinity of the deposited glass, segments of deposited glass were removed from the substrate, crushed, and analyzed by XRD (D8 Advance with DAVINCI, Bruker, GmbH, US). The deposited glass remained amorphous, with no crystallization peaks seen in the XRD patterns. Feedstock glass and deposited glass resulted in comparable XRD patterns.

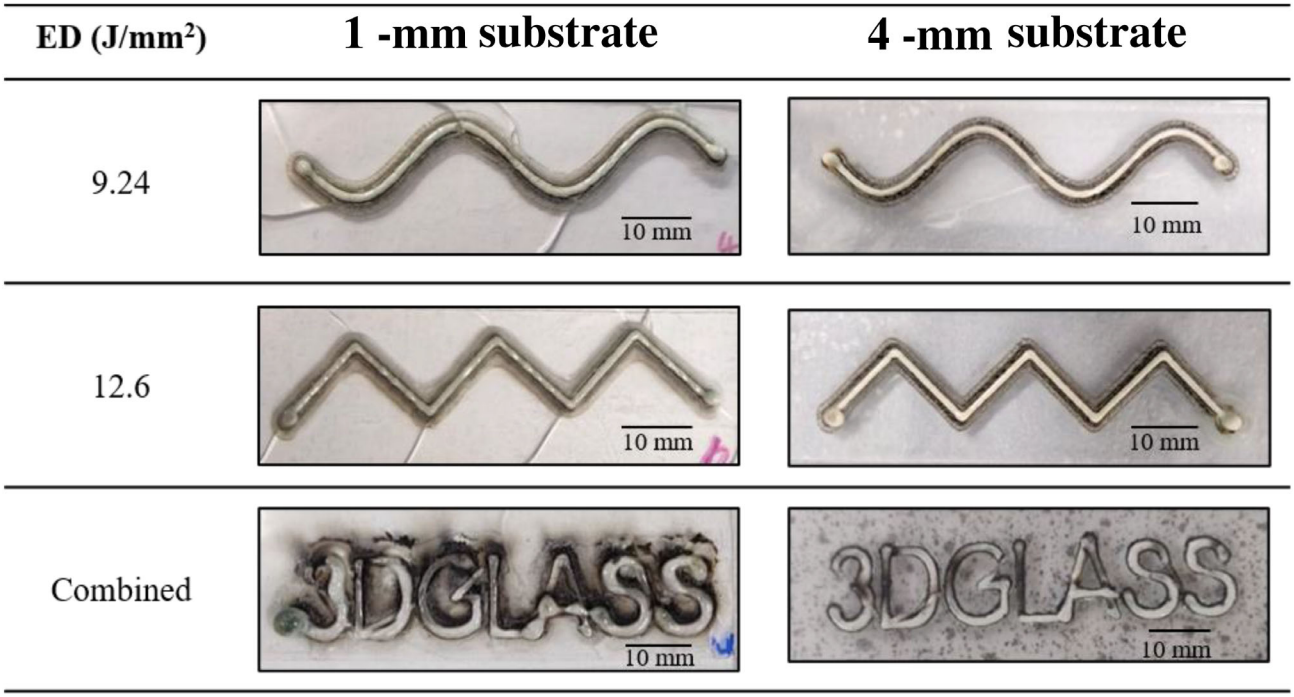

FIGURE 11 Results for processing of different geometries on glass substrates of 1- and 4-mm thickness

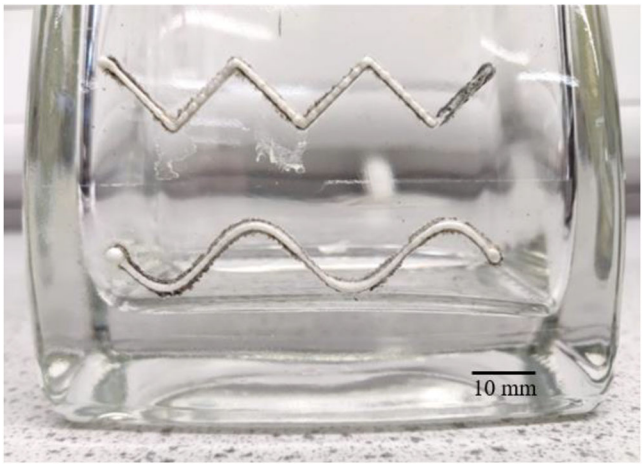

FIGURE 12 Demonstration of processing soda lime silica glass powder onto a bottle surface in different geometries

FTIR spectroscopy was carried out on various regions of the DED glass samples (Frontier FTIR, Perkin Elmer, US). The glass deposit, cellophane tape layer, and black residue were inspected. The resulting spectra confirmed that on laser irradiation, the cellophane tape was vaporized and glass was deposited directly onto the glass substrate. Due to the degradation of the organic tape material, a black carbon residue was also present adjacent to the deposited glass tracks. (Graphical data available in the Supporting Information section).

4 | DISCUSSION

In this study, soda lime silica glass powder was successfully processed by DED for the first time. Suitable parameters were identified for producing consistent glass tracks and structures on glass substrates of different thicknesses, whilst avoiding significant cracking from thermal shock. Feedstock material, delivery system, setup, and laser processing parameters were investigated to allow the processing of glass powder by DED.

The investigation showed that significant consideration of the surface beneath a transparent substrate is vital for achieving sufficient laser absorption for the successful processing of glass powder onto a glass substrate. Reducing the transmittance and reflection of the laser energy and using a heat/energy sink, such as a black anodized base plate, allowed processing by reducing temperature gradients. Adhesion of glass structures was achieved by coating the glass substrate with a layer of cellophane tape prior to processing, which was then vaporized by laser radiation to leave melted glass tracks adhered to the glass substrates. It was also shown that the flowability of a material has a significant impact on powder delivery via nozzles. A well flowing, spherical powder is recommended for processing by this method.

As the focus of these investigations was proving the feasibility of glass processing by this method, substrate modification steps were required. These additional steps are expected to be barriers to commercial application. For

the application of glass bottle décor, matt-black paint was used to coat the inside glass surfaces to improve laser absorption and was later removed with acetone. Alternative methods should be considered to avoid this additional technological step and the introduction of materials that may not be approved for use in these industries. For example, processing on colored glass surfaces, whereby color is imparted from the glass batch, is expected to have improved laser absorption over clear glass substrates. Further optimization of the process is expected to remove the requirement of coating with cellophane tape and darkening glass substrates and may allow consideration of various commercial applications in the future.

The resulting glass deposits varied in the level of opacity, with greater transparency required for the potential decorative applications of this processing method. XRD analysis concluded that there was no crystallization of the glass material, and so the varying opacity is attributed to the presence of bubbles inside deposited glass tracks from glass reboil or the presence of microcracks within the parts or substrates. This is expected to be improved by further optimization of the process, for example, by utilizing a substrate heater to reduce thermal gradients and allow precise control of heating and cooling rate to prevent crack formation, and further optimization of laser parameters to prevent excessive melting of glass feedstocks causing reboil.

A powder feedstock of ~45-μm particle size, and powder delivery parameters of 1 and 2 rpm (wheel speed) at 5 L/min (carrier gas flow), through a side fed nozzle, was found to be most suitable for powder delivery. Powder delivery via lateral nozzle resulted in a consistent delivery of glass at a rate of 39 mg/s, allowing the processing of single-layer structures. Lateral nozzles are easy to use but have been shown to result in varying deposit height dependent on scan direction with relation to the delivery of powder.[26] Although coaxial nozzles do not suffer this effect and are therefore better suited to multilayer processing in comparison, in this study, powder delivery via coaxial nozzle was impeded by the low flowability of the selected glass feedstock and feed rate was insufficient for consistent processing. For multilayer processing, further optimization of powder delivery via coaxial nozzle is recommended.

The experimental setup described in these investigations does not represent the capabilities of superior commercial DED systems. As such, finer optimization could be achieved by utilizing a DED system with integrated controls for simultaneous operation of the laser, stage, and material feed. An additional consideration is potential for material recycling and/or recirculation, to improve the efficiency of the process and reduce the material waste.

Measurement of ED was used to relate laser power and scan speed as a representation of the total energy absorbed during processing. The values used for ED are approximations of the total energy delivered to the substrate but do not reflect the total energy absorbed. Presenting this data as a process map allowed the visualization of the effect of the delivered ED on substrate cracking and consolidation of glass powder. Generally, processing above 115-W laser power was found to cause substrate and deposit cracking, likely caused by thermal shock. In contrast, processing conditions below 11 J/mm^2 frequently resulted in inconsistent consolidation and deposition of glass powder. It is possible that initial glass consolidation is determined by a critical ED being reached, where below this ED glass melting cannot occur. To explain the relationship between high laser power and substrate cracking, it is suggested that despite the compromise in scan speed to provide a particular ED for consolidation, an increased laser power results in a reduction in the time taken to reach a critical ED for processing and, thus, increases the temperature gradients, causing thermal shock.

It was concluded that although ED allows simple assessment of parameter combinations, laser power and scan speed showed independent effects on processing. At various energy densities, results varied across different combinations of laser power and scan speed, despite having the same calculated ED. Further investigation will quantify this difference. Cases that deviated from these general trends were observed during testing. These deviations may be explained by variations in processing conditions, such as inconsistent powder feed, variation in substrate quality, or machine error. Computational modeling of energy absorption during the DED processing of glass materials could allow consideration of significant parameters that are missed in the simple ED calculations and provide a more accurate representation of energy absorption. Future efforts will be made to simulate the effect of laser parameters on glass powder DED to aid the definition of optimal processing conditions. Additionally, due to the many factors that impact glass processing by this method, the process maps generated may only be considered relevant for the exact setup and parameters stated. Process maps present different results dependent on substrate thickness and process design, with other variables such as glass composition and PSD suspected to also have a significant effect on processing windows.

5 | CONCLUSIONS

Novel glass processing by powder-fed directed energy deposition was demonstrated in this investigation.

Key findings include the following:

- Soda lime silica glass spheres were successfully consolidated and deposited on to glass substrates by laser radiation.

- A suitable processing window was found between 11.5 and 12.5 J/mm^2 ED for single-layer processing of soda lime silica tracks onto a 1-mm glass substrate.
- Substrate cracking was observed in parameter combinations where laser power exceeded 115 W, suggesting this should be taken into account when considering a processing window for DED of this glass feedstock.
- A powder delivery rate of 39 mg/s was achieved during feed of spherical soda lime silica powder with an average particle size of 45 μm, through a 2-mm Teflon-lined nozzle.
- A single layer of adhesive tape aided the deposition and adhesion of glass powder onto glass surfaces.
- Laser absorption was improved by utilizing an energy sink beneath transparent substrates.
- Straight, curved, and text features were successfully built on 1 mm, 4 mm, and glass bottle substrates.
- ED indicated the effect of different combinations of laser power and scan speed; however, it was observed that these parameters had independent effects on glass processing by this technique.

Addition of glass décor on glassware and premium glass bottles for brand differentiation is demonstrated as a prospective application of glass DED, offering possibilities for translation of this technology to other applications. Further optimization of the process will help to secure the method as a valid alternative to traditional glass decoration techniques. Reduction of thermal stress and microcrack development in substrates is still required, with investigation into substrate and process heating a promising option for improvement. Single-layer structures, while useful for glass surface decoration, limit the complexity of design in 3D. To address this, future investigations will involve formation of multilayer structures to evaluate the potential of this method for processing glass in three dimensions.

ACKNOWLEDGMENTS

This work was funded by the EPSRC (Engineering and Physical Sciences Research Council, UK) Centre for Doctoral Training in Additive Manufacturing and 3D Printing (Grant no.: EP/L01534X/1). The authors would like to acknowledge additional support and funding from Glass Technology Services (GTS), as well as Stuart Branston and Alexander Jackson-Crisp for technical support, and Ehab Saleh for early experimental help.

ORCID

Ruth Goodridge https://orcid.org/0000-0003-4335-3327

REFERENCES

1. Gugger H. Laser marking of ceramic materials, glazes, glass ceramics and glasses. United States Patent 4769310, 1988.
2. Zhang S, Zeng X, Matthews DTA, Igartua A, Rodriguez-Vidal E, Contreras Fortes J, et al. Selection of micro-fabrication techniques on stainless steel sheet for skin friction. Friction. 2016;4:89–104.
3. Weller C, Kleer R, Piller FT. Economic implications of 3D printing: market structure models in light of additive manufacturing revisited. Int J Prod Econ. 2015;164:43–56.
4. Nguyen DT, Meyers C, Yee TD, Dudukovic NA, Destino JF, Zhu C, et al. 3D-printed transparent glass. Adv Mater. 2017;29:1701181.
5. Dylla-Spears R, Yee TD, Sasan K, Nguyen DT, Dudukovic NA, Ortega JM, et al. 3D printed gradient index glass optics. Sci Adv. 2020;6:eabc7429.
6. Kotz F, Plewa K, Bauer W, Schneider N, Keller N, Nargang T, et al. Liquid glass: a facile soft replication method for structuring glass. Adv Mater. 2016;28:4646–50.
7. Kotz F, Quick AS, Risch P, Martin T, Hoose T, Thiel M, et al. Two-photon polymerization of nanocomposites for the fabrication of transparent fused silica glass microstructures. Adv Mater. 2021;33:e2006341. https://doi.org/10.1002/adma.202006341
8. Klein J. Additive Manufacturing of Optically Transparent Glass. Thesis, Massachusetts Institute of Technology, 2014.
9. Klein J, Stern M, Franchin G, Kayser M, Inamura C, Dave S, et al. Additive manufacturing of optically transparent glass. 3D Print Addit Manuf. 2015;2:92–105.
10. Datsiou KC, Saleh E, Spirrett F, Goodridge R, Ashcroft I, Eustice D. Additive manufacturing of glass with laser powder bed fusion. J Am Ceram Soc. 2019;102:4410–4.
11. Datsiou KC, Spirrett F, Ashcroft I, Magallanes M, Christie S, Goodridge R. Laser powder bed fusion of soda lime silica glass: optimisation of processing parameters and evaluation of part properties. Addit Manuf. 2021;39:101880.
12. Khmyrov RS, Grigoriev SN, Okunkova AA, Gusarov AV. On the possibility of selective laser melting of quartz glass. Physica Procedia. 2014;56:345–56.
13. Vogel W. Structure and crystallization of glasses. Oxford: Pergamon; 1971.
14. Khmyrov RS, Protasov CE, Grigoriev SN, Gusarov AV. Crack-free selective laser melting of silica glass: single beads and monolayers on the substrate of the same material. Int J Adv Manuf Technol. 2016;85:1461–9.
15. Ashby M. Materials and the environment. Oxford: Butterworth-Heinemann; 2013. p. 536–7.
16. Fateri M, Gebhardt A, Thuemmler S, Thurn L. Experimental investigation on selective laser melting of glass. In: Physics procedia. Elsevier BV; 2014. p. 357–64.
17. Fateri M, Gebhardt A. Selective laser melting of soda-lime glass powder. Int J Appl Ceram Technol. 2015;12:53–61.
18. Fateri M, Gebhardt A. Jewelry fabrication via selective laser melting of glass. In: ASME 2014 12th Biennial Conference on Engineering Systems Design and Analysis. American Society of Mechanical Engineers; 2014. https://doi.org/10.1115/ESDA2014-20380
19. Eichler F, Skupin M, Katharina Thurn L, Kasch S, Schmidt T. Operating limits for beam melting of glass materials. MATEC Web Conf. 2019;299:01004.
20. Luo J, Pan H, Kinzel EC. Additive manufacturing of glass. J Manuf Sci Eng J ASME. 2014;136:1–6.
21. Luo J, Gilbert LJ, Qu C, Landers RG, Bristow DA, Kinzel EC. Additive manufacturing of transparent soda-lime glass using

a filament-fed process. J Manuf Sci Eng J ASME. 2017;139:1–8.
22. von Witzendorff P, Pohl L, Suttmann O, Heinrich P, Heinrich A, Zander J, et al. Additive manufacturing of glass: CO2-laser glass deposition printing. Procedia CIRP. 2018;74:272–5.
23. Capps NE, Goldstein JT, Rettschlag K, Sleiman K, Jaeschke P, Kaierle S, et al. Direct laser heating of the filament/substrate interface in digital glass forming. Manuf Lett. 2022;31:106–9.
24. Li PM. Study of the FT4 Powder Rheometer: Comparison of the Test Methods and Optimization of the Protocols. Thesis. Universite de Technologie de Compiegne, 2017.
25. Gibson I, Rosen D, Stucker B. Additive manufacturing technologies. 2nd ed. New York, NY: Springer New York; 2015.
26. Zekovic S, Dwivedi R, Kovacevic R. Numerical simulation and experimental investigation of gas-powder flow from radially symmetrical nozzles in laser-based direct metal deposition. Int J Mach Tools Manuf. 2007;47:112–23.

SUPPORTING INFORMATION

Additional supporting information can be found online in the Supporting Information section at the end of this article.

How to cite this article: Spirrett F, Datsiou KC, Magallanes M, Ashcroft I, Goodridge R. Powder-fed directed energy deposition of soda lime silica glass on glass substrates. J Am Ceram Soc. 2023;106:227–240. https://doi.org/10.1111/jace.18638